Reticular pseudodrusen in late-onset retinal degeneration

Title: Reticular pseudodrusen in late-onset retinal degeneration

Authors (in order): Shyamanga Borooah FRCOphth PhD[1,2*], Vasileios Papastavrou FEBO[3*], Leonardo Lando MD[2,4], Jonathan Han BS[2], Jonathan H. Lin MD PhD[2,5,6], Radha Ayyagari PhD[2], Baljean Dhillon FRCOphth[1], Andrew C. Browning PhD FRCOphth[3]

Affiliations:

1. Centre for Clinical Brain Sciences, School of Clinical Sciences, University of Edinburgh, Edinburgh, UK.
2. Shiley Eye Institute, University of California San Diego, La Jolla, USA.
3. Newcastle Eye Centre, Royal Victoria Infirmary, Newcastle upon Tyne, UK.
4. Department of Ophthalmology, Federal University of Goias, Goiania, Brazil.
5. Departments of Ophthalmology and Pathology, Stanford University, Stanford, USA.
6. Veterans Affairs, Palo Alto Healthcare System, Palo Alto, USA.

*These authors contributed equally to this work.

Financial support:
SB is supported by a Foundation Fighting Blindness Career Development Award.
LL is supported by a Pan-American Association of Ophthalmology Sear Scholarship.
RA is supported by a NIH grant 5R01EY021237-04.
JL is supported by a NIH grant 5R01EY027335.
The sponsors or funding organizations have no role in the design or conduct of this research.

Disclosure: No conflicting interest exists for any author.

This article contains additional online-only material. The following should appear online-only: Figures S1, S2, S3; S4; Table 1.

Author for correspondence:

Dr. Shyamanga Borooah
Shiley Eye Institute
9415 Campus Point Drive,
La Jolla, CA 92093

Phone: +1 (858) 822 2835
Email: sborooah@health.ucsd.edu

ABSTRACT

Purpose: To characterize the association of reticular pseudodrusen (RPD) with late-onset retinal degeneration (L-ORD) using multimodal imaging.

Design: Prospective, two-center, longitudinal case series.

Subjects: Twenty-nine cases with L-ORD.

Methods: All subjects were evaluated within a three-year interval with near-infrared reflectance, fundus autofluorescence, and spectral-domain optical coherence tomography. In addition, a subset of patients also underwent indocyanine green angiography, fundus fluorescein angiography, mesopic microperimetry, and multifocal electroretinography.

Main outcome measures: Prevalence, topographic distribution, and temporal phenotypic changes of RPD in L-ORD.

Results: A total of 29 molecularly confirmed L-ORD cases were included in this prospective study. RPD was detected in 18 cases (62%) at baseline, of which 10 were male. The prevalence of RPD varied with age. The mean age of RPD patients was 57.3±7.2 years. RPD was not seen in cases below the fifth decade (n=3 patients) or in the eighth decade (n=5 patients). RPD were found commonly in the macula with relative sparing of the fovea and were also identified in the peripheral retina. The morphology of RPD changed with follow-up. Two cases (3 eyes) demonstrated RPD regression.

Conclusions: RPD is found frequently in cases with L-ORD and at a younger age than in individuals with AMD. RPD exhibits quick formation and collapse, change in type and morphology with time, relative foveal-sparing, and also has a peripheral retinal location in L-ORD.

INTRODUCTION

The term reticular pseudodrusen (RPD) was first used to describe lesions that formed a "yellow interlacing network 125-250 µm wide" in patients with age-related macular degeneration (AMD).[1] RPD are found between the neural retina and the retinal pigment epithelium (RPE).[2] Multimodal imaging studies have found RPD to be a common feature of early and intermediate AMD[3-7]. RPD have been shown to be an independent risk factor for disease progression to geographic atrophy.[7]

The exact pathogenesis causing RPD development has yet to be established. Changes in choroidal circulation have been associated with RPD.[8,9] Additionally, Bruch's membrane (BM) thickening has also been suggested as a cause of RPD[10,11] with RPD-like structures identified in diseases in which BM thickening is prominent, including pseudoxanthoma elasticum[12], Sorsby fundus dystrophy (SFD)[10,13], adult-onset foveomacular vitelliform dystrophy[14], and IgA nephropathy[15]. Lesions resembling RPD have also been reported in cases of late-onset retinal degeneration (L-ORD) (OMIM 608752).[16] L-ORD is a rare, fully penetrant monogenic macular degeneration with autosomal dominant inheritance resulting from mutations in the gene *C1QTNF5/CTRP5*.[17] *C1QTNF5* is expressed by the RPE and ciliary body within the eye.[18]

L-ORD patients usually complain of symptoms caused by a delay in dark adaptation and nyctalopia by their fifth decade, central vision changes in their sixth decade, and central vision loss by their seventh decade.[19,20] One of the pathological hallmarks is significant BM thickening caused by deposits which extend from the *ora serrata* to the optic nerve.[21-23] L-ORD shares many clinical features with AMD, such as sub-RPE deposits, retinal atrophy, and choroidal neovascularization.[24] Nonetheless, several characteristics distinguish L-ORD from AMD, including a strong family history of visual impairment, the presence of long anteriorly-inserted zonules, early fovea sparing atrophy and, in late stages, the extension of

atrophy into the far periphery.[24-27] Genetic confirmation is useful to provide patients with proper counseling.[28]

In this prospective longitudinal study, we phenotype the RPD-like structures in L-ORD cases using multimodal imaging and functional studies and describe the age-based prevalence RPD.

METHODS

In this prospective, longitudinal, two-center study, patients were recruited between January 2011 and December 2016 at the Princess Alexandra Eye Pavilion, Edinburgh, and the Royal Victoria Infirmary, Newcastle upon Tyne, both in the UK. The study received institutional research board approval from the research ethics committee at the Royal Victoria Infirmary Newcastle (11/NE/0199) and adhered to the tenets of the Declaration of Helsinki. Written informed consent was obtained from all patients. The inclusion criteria were cases with a clinical features of L-ORD identified by two experienced ophthalmologists (BD, AB) and molecular confirmation of the S163R mutation in *C1QTNF5*.[24] Individuals were excluded if aged below eighteen or if they presented with severe media opacities which precluded retinal imaging.

Ophthalmic imaging protocol

All patients underwent ocular examination and fundus imaging using either color fundus (TRC-501X, Topcon medical systems, New Jersey, USA), widefield pseudocolor or 30° multicolor (HRA + OCT Spectralis, Heidelberg Engineering, Heidelberg, Germany) photography. Near infra-red reflectance (NIR-R), scanning laser ophthalmoscopy (SLO) for fundus autofluorescence (FAF) (488nm), and spectral domain optical coherence tomography (SD-OCT) (HRA + OCT Spectralis, Heidelberg Engineering, Heidelberg, Germany) were registered with a 30° field of view. For SD-OCT, volume scans of the posterior pole were taken with automated real-time (ART)=9 (61 scans 9x7.5mm). For FAF images, an ART of at least 20 was considered adequate. All images were captured centered at the fovea.

In selected cases, microperimetry was performed using the Nidek MP1 microperimeter (Nidek Technologies, Padova, Italy), under mesopic light, with a 4-2 threshold strategy, and stimulus Goldman III (200ms). A subset of patients from the series also underwent indocyanine green angiography (ICGA), fundus fluorescein angiography (FFA)

(HRA + OCT Spectralis, Heidelberg Engineering, Heidelberg, Germany), and multifocal ERG (mfERG)(Multifocal Imager V3 system, Scottish Health Innovations Ltd, Glasgow, UK). Electrophysiology tests followed the International Standard for Clinical Electrophysiology of Vision standards and, for the mfERG recordings, a wide field of stimulation (90-degree eccentricity) was used.

Definitions of ocular lesions and data analysis

RPD were defined as a network of yellowish or creamy round structures detected by a retina specialist on color fundus imaging.[29] NIR-R, FAF, and SD-OCT imaging were used to confirm the RPD findings. For NIR-R, RPD were diagnosed if a network of round structures were seen with reduced reflectance and occasionally with increased central reflectance.[10,13] On FAF, the RPD diagnosis was made if a network of rounded structures was identified with reduced autofluorescence and, in some cases, with increased autofluorescence. Finally, on SD-OCT, RPD were diagnosed when an accumulation was noted between the hyperreflective lines representing the RPE-BM complex and the ellipsoid zone. The characteristic RPD findings had to be present in two of the three imaging modalities (NIR-R, FAF, and SD-OCT) similar to a method used in previously published work.[10] Exams were performed at baseline and follow-up consultations within three years. Descriptive statistics were performed using SPSS (Version 25; IBM SPSS Statistics, Chicago, IL, USA).

RESULTS

A total of 29 patients (n=58 eyes) with L-ORD were examined in this study (Table 1, available at https://www.ophthalmologyretina.org). Genetic testing was performed on all participants, revealing the most common mutation associated with L-ORD, the S163R mutation the *C1QTNF5* gene.

Prevalence of RPD in L-ORD at baseline and follow-up

Eighteen (n=36 eyes; 62%) of the 29 L-ORD patients were found to have pseudodrusen in either eye, of which 13 were male (Table 1, available at https://www.ophthalmologyretina.org). The mean age of L-ORD patients with RPD was 57.3±7.2 years, of which 10 were male. In the group without RPD (n=11 patients, 22 eyes; 38%), the mean age was 60.0±15.8 years, 8 being female. The mean follow-up time was 2.15±0.61 years.

Within the RPD group, baseline lesions were most commonly identified in the sixth decade (n=8 patients, 16 eyes; 27.6% of total series, 100% within decade), but were also seen in the fifth decade (n=4 patients, 8 eyes; 13.8% of total series, 75% within decade) and seventh decade (n=10 patients, 20 eyes; 34.5% of total series, 70% within decade) (Figure 1). The youngest patient noted to have RPD was 44 years of age while the eldest was 67 years old. Two patients (6.9% of total series, 11.8% of RPD group) were noted to have unilateral disease only. At three-year follow-up, one patient who initially presented with RPD in both eyes had involution of RPD bilaterally; and another individual manifested RPD regression in one eye. The remainder of the patients who had RPD at baseline (n=17 patients, 33 eyes; 94.4% of patients, 91.7% of eyes) continued to have detectable RPD at follow-up.

L-ORD patients who did not have RPD were divided into a younger subset and an older subset (Figure 1). The younger subset had a mean age of 37.9±3.8 years (n=3 patients, 6 eyes; range, 34-43 years), while the older subset had a mean age of 71.7±4.9 years (n=7 patients,

14 eyes; range, 63-80 years). The younger subset did not have retinal features of L-ORD, but all of the younger subset patients demonstrated clinical features of L-ORD with long anterior zonules. Additionally, they all had a molecular confirmation of L-ORD. None of the patients without initial RPD at baseline developed lesions within three years of follow-up.

Phenotype and topographical distribution of RPD in L-ORD

Color fundus or multicolor imaging in all patients with RPD revealed small yellow or cream-colored spots (Figures 2A-B). Multicolor imaging highlighted pseudodrusen better than color fundus images. NIR-R imaging revealed focal increased NIR-R at the center of RPD with a halo of reduced reflectance surrounding (Figure 2C). Blue and green spectrum imaging demonstrated increased reflectance at the center of pseudodrusen (Figures 2D-E). SD-OCT studies showed an irregular, thickened interdigitating zone (IZ) with a widening of the spacing between the ellipsoid zone (EZ) and the IZ. RPD manifested either as bumps or as peaks appearing to disrupt the EZ and occasionally the external limiting membrane (Figure 2F). The IZ exhibited unclear distinction in regions of RPD in L-ORD, keeping with previous reports from AMD and L-ORD.[16,30,31]

Previous studies had suggested that RPD was associated with BM thickening.[10,13] If RPD were truly associated with BM thickening, one would expect to see RPD not only at the macula but across the entire fundus in L-ORD. As a result, widefield pseudocolor imaging was performed to see whether RPD could be identified peripherally. RPD were identified using this imaging technique and were noted in the periphery in all 18 patients with RPD (Figures 2G-I).

RPD in AMD patients has been classified into types 1-3 depending on the amount of disruption of the EZ.[30] In L-ORD patients, RPD demonstrated a similar morphology to that seen in AMD (Figure S1, available at https://www.ophthalmologyretina.org). All three RPD

types were variably identified in L-ORD eyes, sometimes with different types occurring within the same eye or on a single SD-OCT scan.

Longitudinal change of RPD in L-ORD

In order to better understand L-ORD RPD progression, we performed longitudinal studies to look at SD-OCT with corresponding NIR-R imaging covering a three-year period. Topographical analysis of RPD in AMD has shown that RPD were found at the macula but relatively spared the fovea with a greater propensity for the perifovea, and the superior and temporal arcade vessels.[32,33] We performed a similar analysis in our L-ORD patients using methods previously described to study RPD topography in inherited retinal disease (Figure 3A).[10,13]

RPD in L-ORD were also noted to be relatively reduced at the fovea compared to surrounding areas. Forty-four percent of L-ORD eyes with RPD at baseline (n=9 patients, 16 eyes) were found to have RPD at the fovea (Figure 3B). At follow-up, foveal RPD was encountered in 58% of eyes from the RPD group (n=12 patients, 21 eyes) (Figure 3C). In the group who did not present with RPD at baseline, no new eyes evolved with foveal lesions within three-years of follow-up.

The most common area for RPD were the temporal zones, followed by the inferior, superior, and nasal zones. After three years of follow-up, lesions assumed a more distributed pattern, yet kept the same overall order of prevailing distribution.

A gradual increase in RPD from the temporal to the nasal macula was noted with relative foveal sparing (Figure 4A). The RPD showed rapid evolution within three years of follow-up and different patterns of change. RPD which were initially very punctate at baseline, with normal NIR-R reflectance in a round/ovoid center surrounded by a halo of reduced reflectance, corresponded with SD-OCT findings of type 3 RPD (Figure 4A). Within a year, some RPD were noted to change from type 3 to type 1 and 2 RPD (Figure 4C) (Figure S2,

available at https://www.ophthalmologyretina.org). Some regions with RPD were associated with localized or extensive outer retinal atrophy (Figure 4D). NIR-R showed more reticular lesions associated with the type 1 RPD. In the same region, but not in the same location, new stage 3 RPD were also noted to develop adjacent to the previous stage 3 RPD. Taken together, imaging of RPD in L-ORD demonstrates rapid morphological flux (Figure 4B).

Angiographic findings in eyes with RPD in L-ORD

Retinal and choroidal vascular angiography has previously been used to help refine the phenotype of RPD in AMD.[3,34,35] It has previously been suggested that RPD form at choroidal vascular watersheds.[33] As a result, combined FFA and ICGA were reviewed from a subset of L-ORD patients with RPD who were imaged to exclude choroidal neovascularization after complaining of relatively rapid recent changes to their vision (n=6 patients, 12 eyes; 20.7% of total series, 33.3% of RPD group). FFA revealed RPD in the late phase as hypofluorescent spots which were more clearly seen in areas of hyperfluorescent staining associated with sub-RPE deposit in the temporal region in patients without atrophic disease (Figure S3, available at https://www.ophthalmologyretina.org). These areas corresponded to RPD lesions seen on NIR-R reflectance (Figure S3, available at https://www.ophthalmologyretina.org). Early ICGA was unremarkable. RPD were more easily identified in late stage ICGA and demonstrated discrete areas of hypofluorescence which corresponded with RPD on NIR-R (Figure S3, available at https://www.ophthalmologyretina.org). Mid-late ICG also highlighted an island in the region of the fovea which was clear of RPD in patients in L-ORD patients with early non-atrophic disease (Figure S3, available at https://www.ophthalmologyretina.org). ICGA did not demonstrate any clear correspondence between the location of RPD and choroidal vascular watersheds.

Functional changes in eyes with RPD in L-ORD

One of the earliest symptoms experienced by L-ORD patients is nyctalopia. To investigate whether RPD in L-ORD are associated with any functional changes, we performed microperimetry, and mfERG in three individuals with clinical disease who had no signs of atrophy confirmed by FAF imaging. All three patients complained of symptoms of nyctalopia. Microperimetry showed reduced sensitivity temporally which corresponded with areas of reduced mfERG waveform amplitudes. All three patients exhibited some reduction in response in regions with dense pseudodrusen using microperimetry and mfERG (Figure 5). The multifocal ERG primarily measures cone photoreceptor response under light-adapted conditions.[36] The full-field ERGs in these patients, performed following 20 minutes of dark adaptation, showed a reduced rod response with relative preservation of overall of cone function (Figure S4, available at https://www.ophthalmologyretina.org). The microperimetry and mfERG findings in the context of the normal SD-OCT thickness findings suggest that localized cone and more generalized rod dysfunction, rather than degeneration, may occur in the presence of RPD.

DISCUSSION

This article presents findings from a natural history study of L-ORD patients using multimodal imaging. The RPD phenotype is commonly seen in L-ORD using multimodal imaging. The prevalence of RPD in L-ORD in our series was 62% and it was seen in 18 of the 29 L-ORD patients included in this study at baseline. RPD was most commonly seen in the sixth decade when all patients within this age group were noted to have RPD. However, there was a window for RPD occurrence in L-ORD between the fifth and seventh decades. These findings in L-ORD contrast with AMD which has a later onset and where RPD prevalence increases with age.[37,38] The prevalence of RPD in AMD has been found to vary between 13.4% and 52% using multimodal imaging.[3-6] However, RPD prevalence also varied with the stage of AMD, being highest in intermediate AMD and declining in end stage AMD including geographic atrophy.[39,40] The prevalence of RPD in L-ORD was closer to other inherited macular degenerations, such as SFD.[13] In SFD patients, RPD were only encountered in the sixth decade in 71% of cases (n=7) and were not seen at older ages.

There have been a number of previous clinical reports of L-ORD patients. The majority of the early studies primarily used color fundus photography for phenotyping and have alluded to RPD describing drusenoid changes which match the description of RPD described in the present paper.[20,22,26] Some later studies have also used multimodal imaging which have included SD-OCT, NIR-R and FAF in some series of patients who had previously been included earlier studies were re-examined using different modalities.[16,26,27,41] However, it is only relatively recently that RPD-like lesions have been localized to the sub-retina using a combination of NIR-R and SD-OCT.[16]

It has been suggested that RPD in AMD form in areas of poor choroidal circulation such as choroidal watershed regions.[33] In our study six ICGs were performed in L-ORD patients. RPD were clearly seen in mid to late phase of all patients, which is similar to the findings of

100% sensitivity in AMD cases.[3] However, we did not find a localization to choroidal lobules.

RPD have also been associated with BM thickening. This is supported by studies in other retinal diseases such as pseudoxanthoma elasticum in which the RPD were seen in areas of BM thickening.[10] One of the pathological hallmarks of L-ORD is a thick sub-RPE deposit, which extends from the optic nerve to the *ora serrata*.[23] In L-ORD, a thickening of the inner collagenous layer of BM, which has previously been identified using electron microscopy and BM thickness measurements in histopathology samples from L-ORD patients with advanced disease, have measured the BM to be approximately 50µm thick.[17,22,23] If RPD resulted from BM thickening alone, it would be expected that the whole of the retina would be covered by RPD in L-ORD. In the present paper, we show evidence for RPD not only at the macula but also in the far periphery. This suggests that BM thickening may be associated with RPD formation. The identification of far peripheral RPD appears different from the reports of RPD in AMD[42,43].

The topographical studies in this paper showed that RPD relatively spared the fovea. This also confirms the findings regarding RPD in the single previous study describing the long term follow-up of 2 siblings affected by L-ORD.[16] This study examined the patients for more than eight years and found that RPD-like lesions which started temporally then progressed nasally sparing the fovea. The topographical findings in our study suggest that RPD have a propensity to occur in rod-rich areas of the fundus and are relatively reduced in the fovea, which has a higher density of cones. This points to the fact that RPD formation in L-ORD may be linked to rod photoreceptor pathophysiology. In the present study we identify photoreceptor dysfunction associated with RPD but it is unclear whether photoreceptor dysfunction is causal in RPD formation. This may be resolved if the younger cases which currently have no RPD have longitudinal electrophysiological follow-up. Our findings of rod

297 dysfunction associated with RPD in L-ORD are similar to the conclusions of previous studies
298 which indicate that rods are affected prior to cones in L-ORD in human and animal
299 studies.[20,23,26,27,44]
300 RPD-like lesions have also been seen in vitamin A deficiency and have a similar foveal
301 sparing pattern.[45] The similarity in phenotype with vitamin A deficiency suggests that
302 dysfunctional vitamin A recycling may play a role in RPD formation. Additionally, rod
303 dysfunction in L-ORD is greater than can be accounted for by cell loss alone[41] and prolonged
304 dark adaptation improves rod photoreceptor response in L-ORD suggesting that rod
305 photoreceptor dysfunction predominates over cell loss in the early stages of L-ORD.[46] High-
306 dose vitamin A treatment in L-ORD has also shown some improvement of dark adaptation
307 kinetics.[20,25] However, these studies did not look at the effect of vitamin A treatment on RPD.
308 It would be interesting to investigate the effect of high dose vitamin A on RPD in L-ORD.
309 Although the present paper describes the findings from one of the largest series of L-ORD
310 patients, some limitations still occur from the relatively small number of patients at different
311 ages, an inherent challenge when studying such rare conditions. We also acknowledge that
312 the limited number of complimentary functional tests performed on some cases and the lack
313 of standardization of genetic tests.
314 The studies presented in this paper help refine the RPD phenotype of L-ORD using a
315 longitudinal follow-up of a large series of patients using multimodal imaging and describe
316 RPD changes with time in L-ORD. In addition, the presented studies outline RPD prevalence
317 with age in L-ORD and help quantify RPD topography at the macula and changes with time.
318

ACKNOWLEDGEMENTS

Acknowledgements to the assistance of the staff at the Shared University Research Facilities (SuRF) at the University of Edinburgh and Dr. Nissi Varki in the Department of Pathology, University of California San Diego. In addition, we would like to thank the assistance of Mark Hope and Marion McClure in the medical photography department Princess Alexandra Eye Pavilion and the electrophysiology department at the Tennent Institute of Ophthalmology, Gartnavel General Hospital, Glasgow for mfERG studies.

ABBREVIATIONS

AMD: age-related macular degeneration

ART: automated real time

BM: Bruch's membrane

ETDRS: Early Treatment Diabetic Retinopathy Study

EZ: ellipsoid zone

FAF: fundus autofluorescence

FFA: fundus fluorescein angiography

ICGA: indocyanine green angiography

IZ: interdigitating zone

L-ORD: late-onset retinal degeneration

mfERG: multifocal electroretinography

NIR-R: Near infra-red reflectance

RPD: reticular pseudodrusen

RPE: retinal pigment epithelium

SD-OCT: spectral domain optical coherence tomography

SFD: Sorsby macular dystrophy

SLO: scanning laser ophthalmoscopy

References

1. Arnold JJ, Sarks SH, Killingsworth MC, Sarks JP. Reticular pseudodrusen. A risk factor in age-related maculopathy. *Retina.* 1995;15(3):183-191.
2. Sarks JP, Sarks SH, Killingsworth MC. Evolution of geographic atrophy of the retinal pigment epithelium. *Eye (Lond).* 1988;2 (Pt 5):552-577.
3. Ueda-Arakawa N, Ooto S, Tsujikawa A, Yamashiro K, Oishi A, Yoshimura N. Sensitivity and specificity of detecting reticular pseudodrusen in multimodal imaging in Japanese patients. *Retina.* 2013;33(3):490-497.
4. De Bats F, Mathis T, Mauget-Faysse M, Joubert F, Denis P, Kodjikian L. Prevalence of Reticular Pseudodrusen in Age-Related Macular Degeneration Using Multimodal Imaging. *Retina.* 2016;36(1):46-52.
5. Wilde C, Patel M, Lakshmanan A, Morales MA, Dhar-Munshi S, Amoaku WM. Prevalence of reticular pseudodrusen in eyes with newly presenting neovascular age-related macular degeneration. *Eur J Ophthalmol.* 2016;26(2):128-134.
6. Wu Z, Ayton LN, Luu CD, Baird PN, Guymer RH. Reticular Pseudodrusen in Intermediate Age-Related Macular Degeneration: Prevalence, Detection, Clinical, Environmental, and Genetic Associations. *Invest Ophthalmol Vis Sci.* 2016;57(3):1310-1316.
7. Zarubina AV, Neely DC, Clark ME, et al. Prevalence of Subretinal Drusenoid Deposits in Older Persons with and without Age-Related Macular Degeneration, by Multimodal Imaging. *Ophthalmology.* 2016;123(5):1090-1100.
8. Spaide RF. Outer retinal atrophy after regression of subretinal drusenoid deposits as a newly recognized form of late age-related macular degeneration. *Retina.* 2013;33(9):1800-1808.
9. Alten F, Heiduschka P, Clemens CR, Eter N. Exploring choriocapillaris under reticular pseudodrusen using OCT-Angiography. *Graefes Arch Clin Exp Ophthalmol.* 2016;254(11):2165-2173.
10. Gliem M, Hendig D, Finger RP, Holz FG, Charbel Issa P. Reticular pseudodrusen associated with a diseased bruch membrane in pseudoxanthoma elasticum. *JAMA Ophthalmol.* 2015;133(5):581-588.
11. Pauleikhoff D, Harper CA, Marshall J, Bird AC. Aging changes in Bruch's membrane. A histochemical and morphologic study. *Ophthalmology.* 1990;97(2):171-178.
12. Gliem M, Muller PL, Birtel J, Hendig D, Holz FG, Charbel Issa P. Frequency, Phenotypic Characteristics and Progression of Atrophy Associated With a Diseased Bruch's Membrane in Pseudoxanthoma Elasticum. *Invest Ophthalmol Vis Sci.* 2016;57(7):3323-3330.
13. Gliem M, Muller PL, Mangold E, et al. Reticular Pseudodrusen in Sorsby Fundus Dystrophy. *Ophthalmology.* 2015;122(8):1555-1562.
14. Wilde C, Lakshmanan A, Patel M, Morales MU, Dhar-Munshi S, Amoaku WM. Prevalence of reticular pseudodrusen in newly presenting adult onset foveomacular vitelliform dystrophy. *Eye (Lond).* 2016;30(6):817-824.
15. Lally DR, Baumal C. Subretinal drusenoid deposits associated with complement-mediated IgA nephropathy. *JAMA Ophthalmol.* 2014;132(6):775-777.
16. Cukras C, Flamendorf J, Wong WT, Ayyagari R, Cunningham D, Sieving PA. Longitudinal Structural Changes in Late-Onset Retinal Degeneration. *Retina.* 2016;36(12):2348-2356.
17. Hayward C, Shu X, Cideciyan AV, et al. Mutation in a short-chain collagen gene, CTRP5, results in extracellular deposit formation in late-onset retinal degeneration: a

genetic model for age-related macular degeneration. *Hum Mol Genet.* 2003;12(20):2657-2667.
18. Mandal MN, Vasireddy V, Reddy GB, et al. CTRP5 is a membrane-associated and secretory protein in the RPE and ciliary body and the S163R mutation of CTRP5 impairs its secretion. *Invest Ophthalmol Vis Sci.* 2006;47(12):5505-5513.
19. Ayyagari R, Griesinger IB, Bingham E, Lark KK, Moroi SE, Sieving PA. Autosomal dominant hemorrhagic macular dystrophy not associated with the TIMP3 gene. *Archives of ophthalmology.* 2000;118(1):85-92.
20. Jacobson SG, Cideciyan AV, Wright E, Wright AF. Phenotypic marker for early disease detection in dominant late-onset retinal degeneration. *Invest Ophthalmol Vis Sci.* 2001;42(8):1882-1890.
21. Duvall J, McKechnie NM, Lee WR, Rothery S, Marshall J. Extensive subretinal pigment epithelial deposit in two brothers suffering from dominant retinitis pigmentosa. A histopathological study. *Graefes Arch Clin Exp Ophthalmol.* 1986;224(3):299-309.
22. Kuntz CA, Jacobson SG, Cideciyan AV, et al. Sub-retinal pigment epithelial deposits in a dominant late-onset retinal degeneration. *Invest Ophthalmol Vis Sci.* 1996;37(9):1772-1782.
23. Milam AH, Curcio CA, Cideciyan AV, et al. Dominant late-onset retinal degeneration with regional variation of sub-retinal pigment epithelium deposits, retinal function, and photoreceptor degeneration. *Ophthalmology.* 2000;107(12):2256-2266.
24. Borooah S, Collins C, Wright A, Dhillon B. Late-onset retinal macular degeneration: clinical insights into an inherited retinal degeneration. *Br J Ophthalmol.* 2009;93(3):284-289.
25. Ayyagari R, Mandal MN, Karoukis AJ, et al. Late-onset macular degeneration and long anterior lens zonules result from a CTRP5 gene mutation. *Invest Ophthalmol Vis Sci.* 2005;46(9):3363-3371.
26. Vincent A, Munier FL, Vandenhoven CC, Wright T, Westall CA, Heon E. The characterization of retinal phenotype in a family with C1QTNF5-related late-onset retinal degeneration. *Retina.* 2012;32(8):1643-1651.
27. Soumplis V, Sergouniotis PI, Robson AG, et al. Phenotypic findings in C1QTNF5 retinopathy (late-onset retinal degeneration). *Acta Ophthalmol.* 2013;91(3):e191-195.
28. Borooah S, Stanton CM, Marsh J, et al. Whole genome sequencing reveals novel mutations causing autosomal dominant inherited macular degeneration. *Ophthalmic Genet.* 2018;39(6):763-770.
29. Zweifel SA, Imamura Y, Spaide TC, Fujiwara T, Spaide RF. Prevalence and significance of subretinal drusenoid deposits (reticular pseudodrusen) in age-related macular degeneration. *Ophthalmology.* 2010;117(9):1775-1781.
30. Zweifel SA, Spaide RF, Curcio CA, Malek G, Imamura Y. Reticular pseudodrusen are subretinal drusenoid deposits. *Ophthalmology.* 2010;117(2):303-312 e301.
31. Khan KN, Borooah S, Lando L, et al. Quantifying the Separation Between the Retinal Pigment Epithelium and Bruch's Membrane using Optical Coherence Tomography in Patients with Inherited Macular Degeneration. *Translational Vision Science & Technology.* 2020;9(6):26-26.
32. Curcio CA, Messinger JD, Sloan KR, McGwin G, Medeiros NE, Spaide RF. Subretinal drusenoid deposits in non-neovascular age-related macular degeneration: morphology, prevalence, topography, and biogenesis model. *Retina.* 2013;33(2):265-276.
33. Alten F, Clemens CR, Heiduschka P, Eter N. Localized reticular pseudodrusen and their topographic relation to choroidal watershed zones and changes in choroidal volumes. *Invest Ophthalmol Vis Sci.* 2013;54(5):3250-3257.

34. Querques G, Querques L, Forte R, Massamba N, Coscas F, Souied EH. Choroidal changes associated with reticular pseudodrusen. *Invest Ophthalmol Vis Sci.* 2012;53(3):1258-1263.
35. Sivaprasad S, Bird A, Nitiahpapand R, et al. Perspectives on reticular pseudodrusen in age-related macular degeneration. *Surv Ophthalmol.* 2016;61(5):521-537.
36. Hood DC, Bach M, Brigell M, et al. ISCEV standard for clinical multifocal electroretinography (mfERG) (2011 edition). *Doc Ophthalmol.* 2012;124(1):1-13.
37. Finger RP, Chong E, McGuinness MB, et al. Reticular Pseudodrusen and Their Association with Age-Related Macular Degeneration: The Melbourne Collaborative Cohort Study. *Ophthalmology.* 2016;123(3):599-608.
38. Joachim N, Mitchell P, Rochtchina E, Tan AG, Wang JJ. Incidence and progression of reticular drusen in age-related macular degeneration: findings from an older Australian cohort. *Ophthalmology.* 2014;121(4):917-925.
39. Zhang Y, Wang X, Sadda SR, et al. Lifecycles of Individual Subretinal Drusenoid Deposits and Evolution of Outer Retinal Atrophy in Age-Related Macular Degeneration. *Ophthalmol Retina.* 2020;4(3):274-283.
40. Chan H, Cougnard-Gregoire A, Delyfer MN, et al. Multimodal Imaging of Reticular Pseudodrusen in a Population-Based Setting: The Alienor Study. *Invest Ophthalmol Vis Sci.* 2016;57(7):3058-3065.
41. Jacobson SG, Cideciyan AV, Sumaroka A, Roman AJ, Wright AF. Late-onset retinal degeneration caused by C1QTNF5 mutation: sub-retinal pigment epithelium deposits and visual consequences. *JAMA Ophthalmol.* 2014;132(10):1252-1255.
42. Hogg RE, Silva R, Staurenghi G, et al. Clinical characteristics of reticular pseudodrusen in the fellow eye of patients with unilateral neovascular age-related macular degeneration. *Ophthalmology.* 2014;121(9):1748-1755.
43. Lee MY, Yoon J, Ham DI. Clinical features of reticular pseudodrusen according to the fundus distribution. *Br J Ophthalmol.* 2012;96(9):1222-1226.
44. Chavali VR, Khan NW, Cukras CA, Bartsch DU, Jablonski MM, Ayyagari R. A CTRP5 gene S163R mutation knock-in mouse model for late-onset retinal degeneration. *Hum Mol Genet.* 2011;20(10):2000-2014.
45. Aleman TS, Garrity ST, Brucker AJ. Retinal structure in vitamin A deficiency as explored with multimodal imaging. *Doc Ophthalmol.* 2013;127(3):239-243.
46. Papastavrou VT, Bradshaw KR, Aye KH, Turney C, Browning AC. Improvement of retinal function in L-ORD after prolonged dark adaptation. *Can J Ophthalmol.* 2015;50(2):112-118.

FIGURE LEGENDS

Figure 1. Prevalence of reticular pseudodrusen in late-onset retinal degeneration with age at baseline.

Figure 2. Fundus imaging of reticular pseudodrusen (RPD) in a 61-year-old late onset retinal degeneration patient. (A) Color fundus photograph from the right eye displays discrete yellowish spots around the macula with foveal sparing. (B) Spectralis merged multicolor image from the superior macula demonstrating yellow discrete lesions surrounded by a darkened halo. Similar findings of increased reflectance centrally surrounded by a halo of reduced reflectance are seen in the infra-red (C), green (D), and the blue reflectance (E) with white arrowheads highlighting corresponding RPD. (F) SD-OCT imaging through the same region as figures B-E shows the neuroretina with a mainly intact external limiting membrane and ellipsoid zone occasionally interrupted by RPD (white arrowheads). (G) Widefield pseudocolor peripheral fundus imaging from a 54-year-old male patient reveals reticular lesions in the peripheral fundus. (H-I) Magnified frames better demonstrate the reticular pattern of lesions.

Figure 3. Late-onset retinal degeneration (L-ORD) reticular pseudodrusen (RPD) topography changes. (A) Representative NIR-R fundus image from a 57-year-old L-ORD patient with RPD. A modified Early Treatment Diabetic Retinopathy Study (ETDRS) grid which subdivided the posterior fundus into 15 areas was overlaid and centered on the fovea on the NIR-R images to assess the topographic distribution of RPD. Left eyes were converted so that the temporal hemi-field is represented on the right-hand side for both eyes. (B) The percentages represent the frequency of RPD in each ETDRS sector of all L-ORD eyes which manifested RPD at baseline (n=18 patients, 34 eyes). (C) A grid analyzing this same RPD group detected lesions in the majority of eyes within three years of follow-up (n=17 patients, 33 eyes).

Figure 4. Longitudinal changes observed in four different late-onset retinal degeneration (L-ORD) patients. (A) Baseline (A') and follow-up (A'') spectral domain optical coherence tomography (SD-OCT) from the left eye of a 45-year-old female displays reticular pseudodrusen (RPD) progression, as seen by expansion and new onset (brackets), after approximately two years. The white oval which represents relative foveal sparing initially (A') is lost at follow-up (A''). On the temporal side, a cluster of mostly type 2 and 3 RPD (A', arrows) evolves with deformation, regression, and degeneration (A'', arrows), with relative preservation of the outer retinal layers. (B) Right-eye SD-OCT scans from a 60-year-old female illustrates RPD remodeling and lesions advancement from baseline (B', arrows) with three-year follow-up (B'', bracket). This patient's retinal findings evolved from RPD with preservation of outer retinal structures and no atrophy (B') to early atrophic disease (B'') as seen on the NIR-R. (C) SD-OCT scans taken approximately two years apart in a 51-year-old female showcase a frequent finding in RPD: the progression to atrophy at the site of previous lesions. In this case, the arrowheads indicate corresponding RPD points at baseline (C') which became atrophic (C'') following RPD breakdown. The outer retinal layers are lost and the overlying retina starts to collapse down in this area. (D) An example of rapid RPD (D', bracket) transformation into extensive atrophy (D'', bracket) following disease progression from minimally atrophic to predominantly atrophic regions in the left eye of a 62-year-old male patient with L-ORD after three years.

Figure 5. Visual function assessment from the 58-year-old (A), 62-year-old (B), and 51-year-old individuals. On the upper part of each framed case, the optical coherence tomography thickness maps indicate a lack of marked neuroretinal structural loss, despite diminished response in several retinal points as shown by the multifocal electroretinography trace report (middle two rows) and reduced sensitivity on the microperimetry color maps (bottom row).

SUPPLEMENTARY TABLES

Table S1. Summary of late-onset retinal degeneration cohort patients investigated in this study.

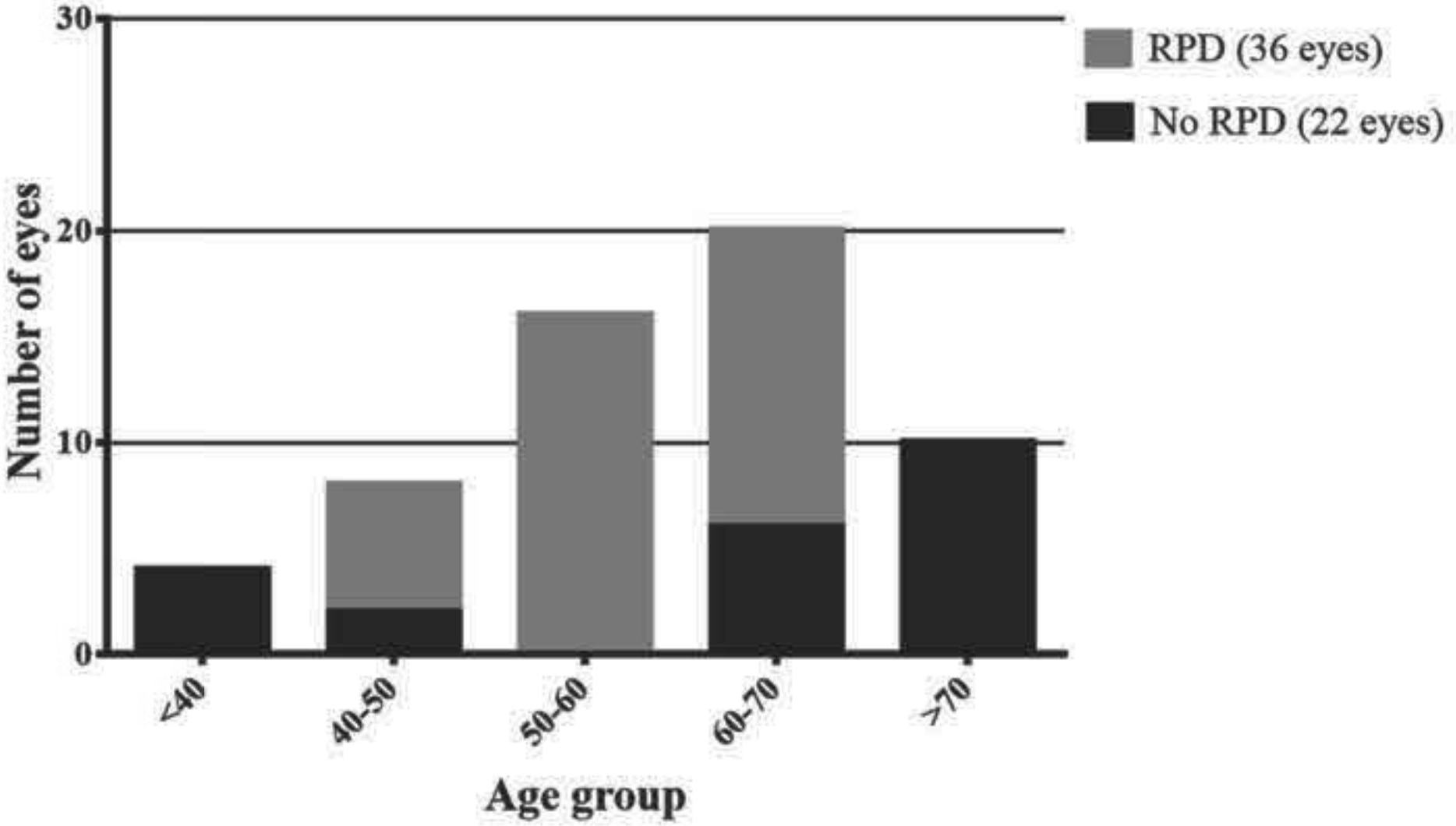

Figure 2

Click here to access/download;Figure;Figure_2.tif

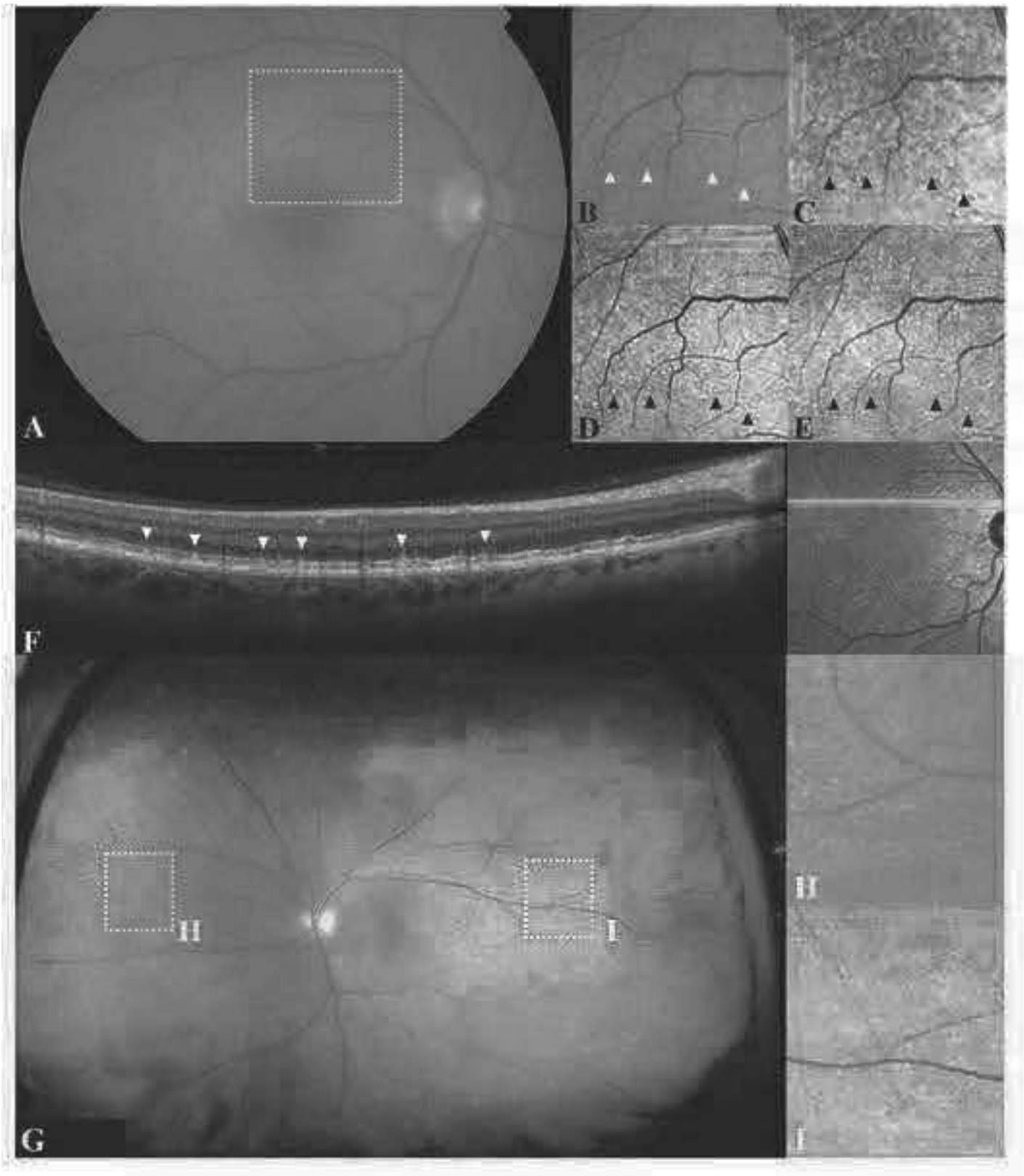

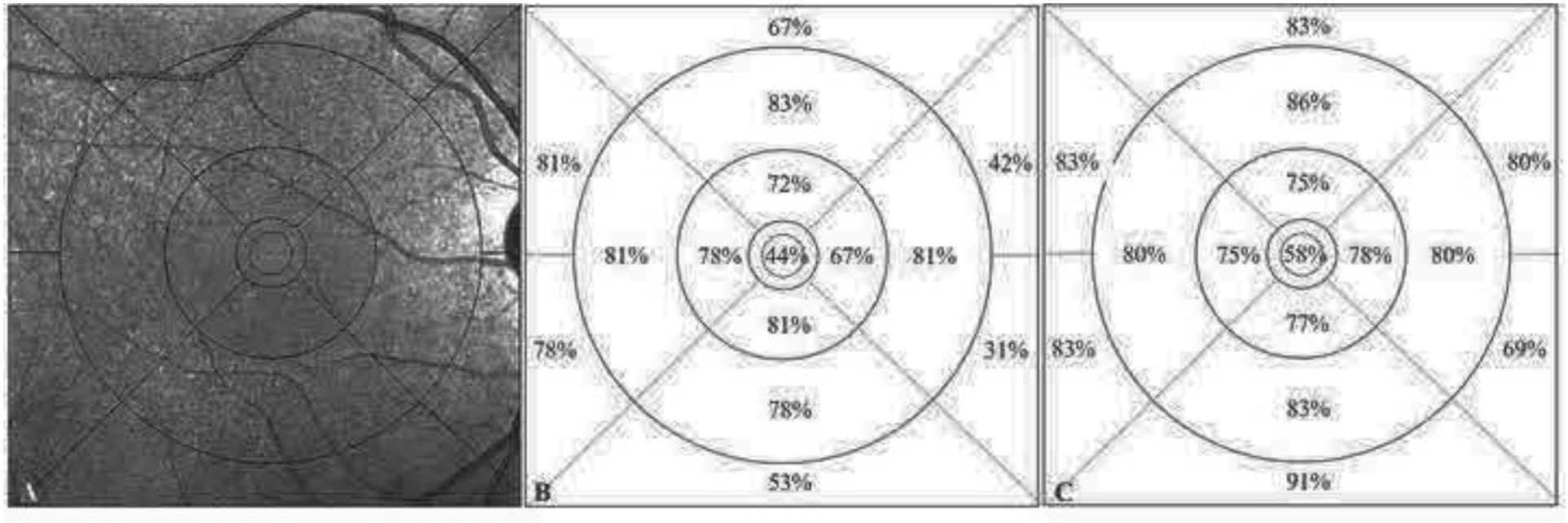

Figure 4

Click here to access/download;Figure;Figure_4.tif

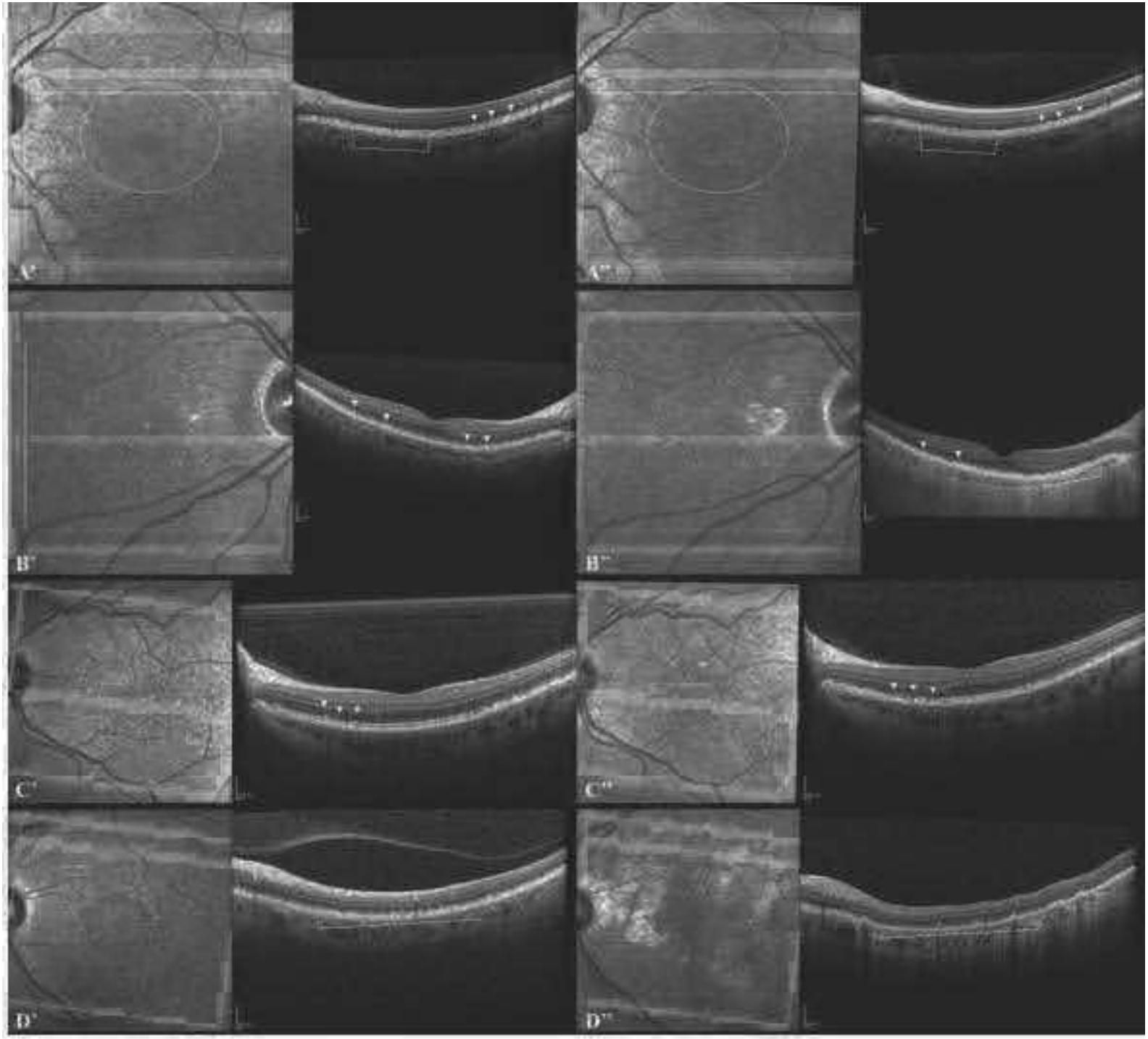

Figure 5

Click here to access/download;Figure;Figure_5.tif

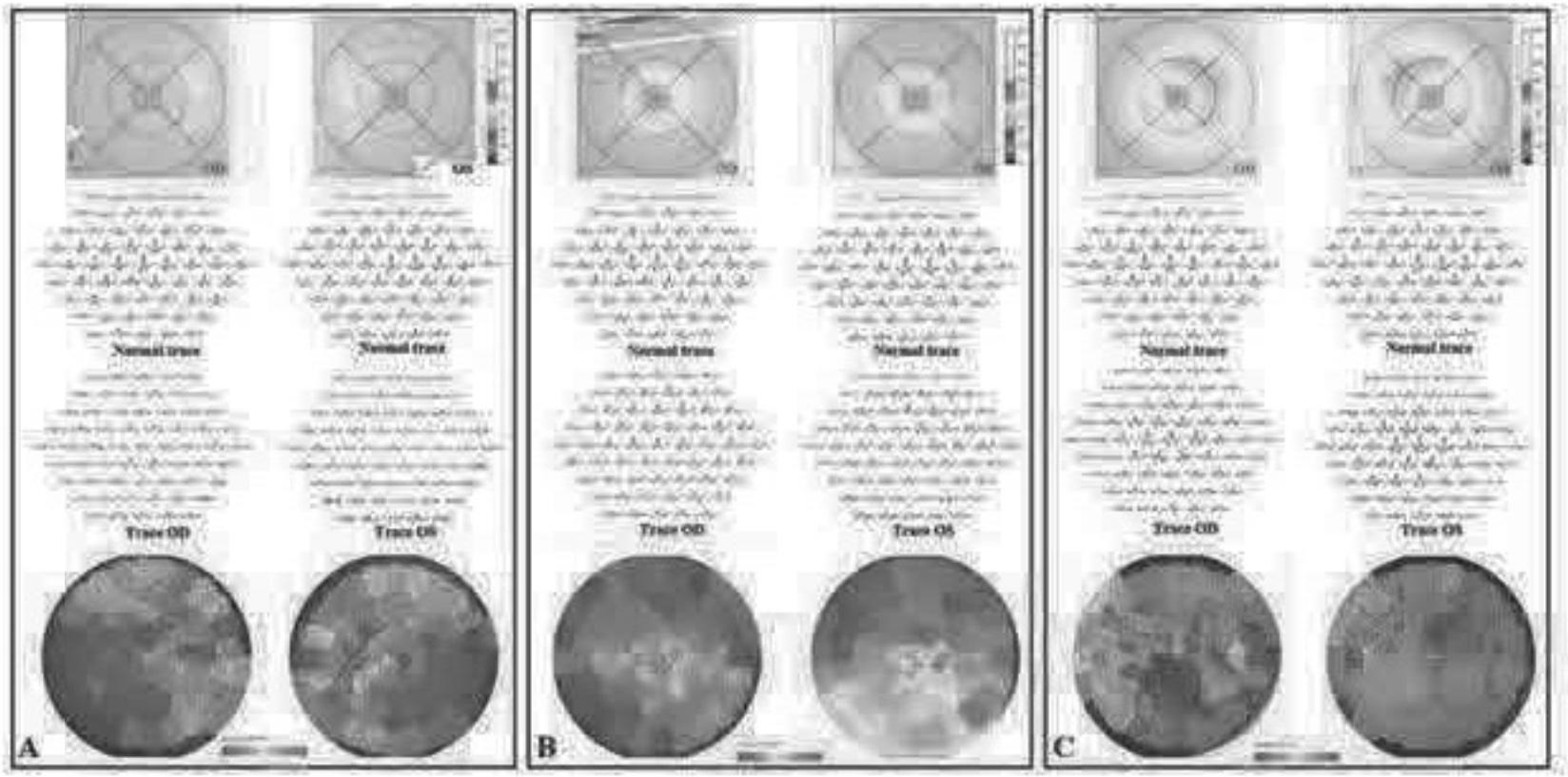

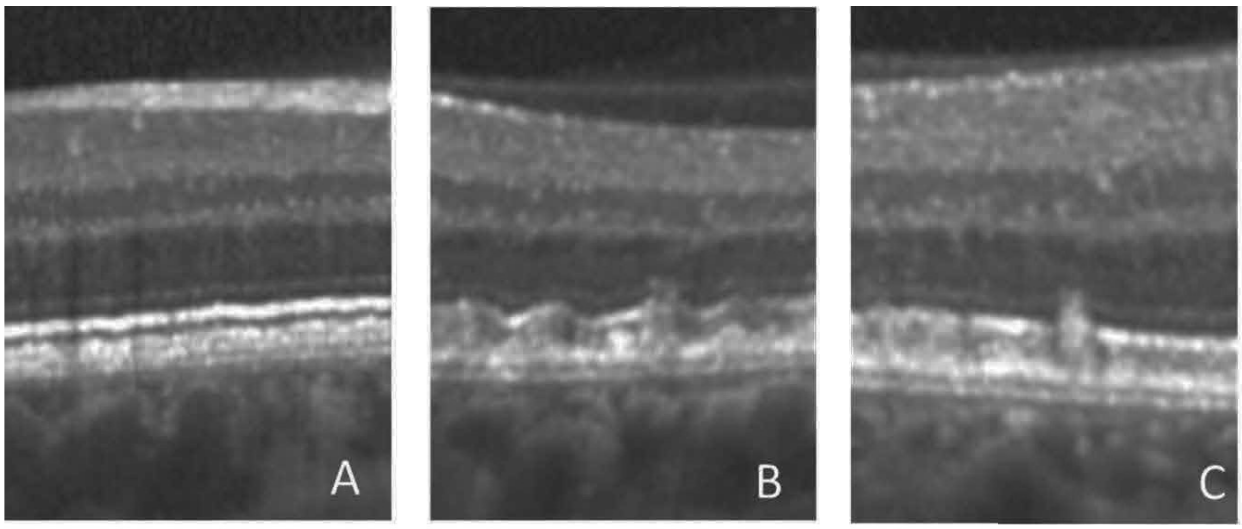

Figure S1. Reticular pseudodrusen (RPD) detected in three different patients with late-onset retinal degeneration by spectral domain optical coherence tomography imaging. The figure exemplifies type 1 (A), type 2 (B), and type 3 (C) RPD.

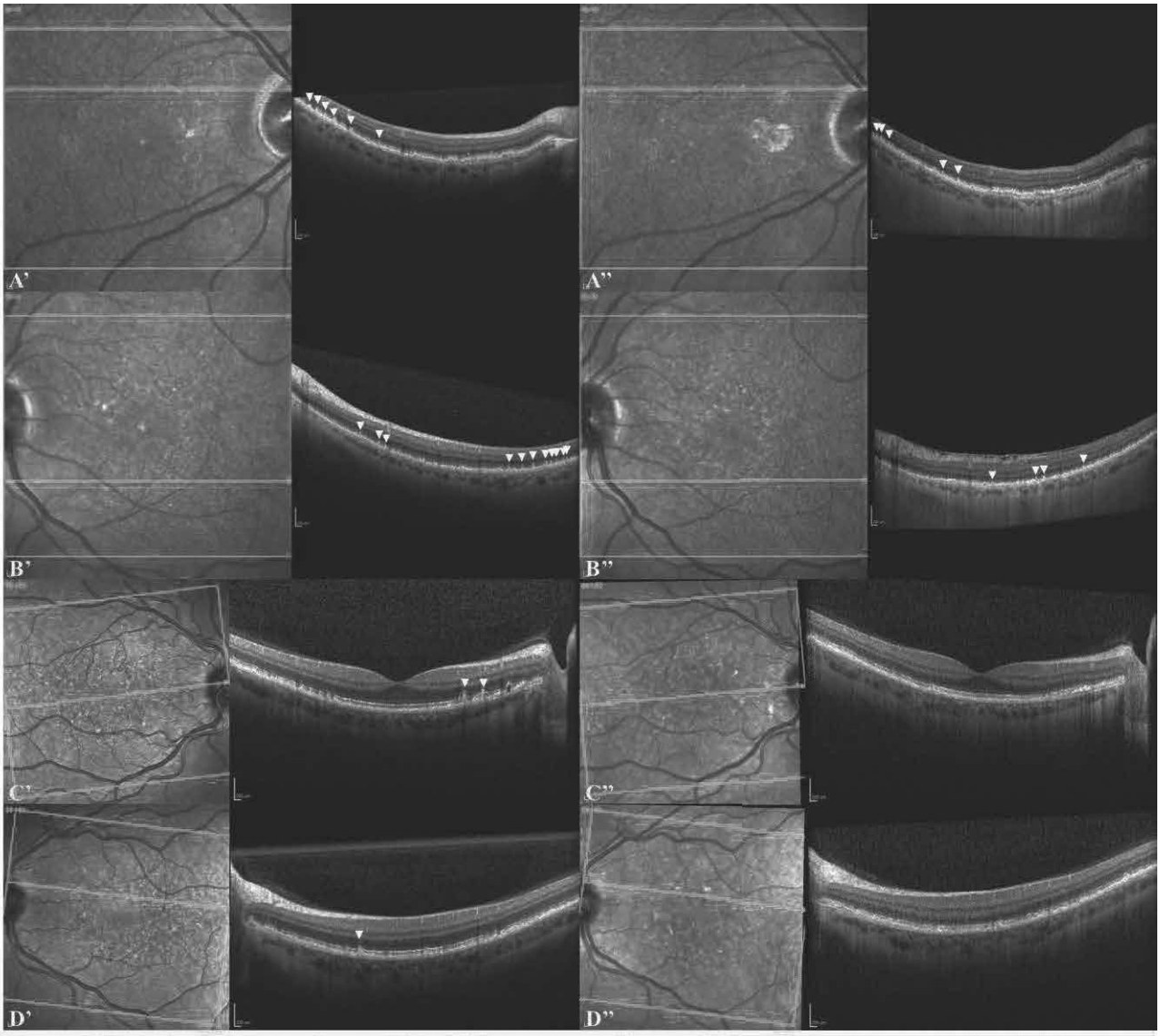

Figure S2. Retinal pseudodrusen changes bilaterally in two cases, a 51-year-old (A and B) and 60-year-old (C and D) females, further exemplify lesions (arrows) which were initially classified as type 3 evolving to type 1. In most of the cases, the external limiting membrane is find preserved after lesions downgrade.

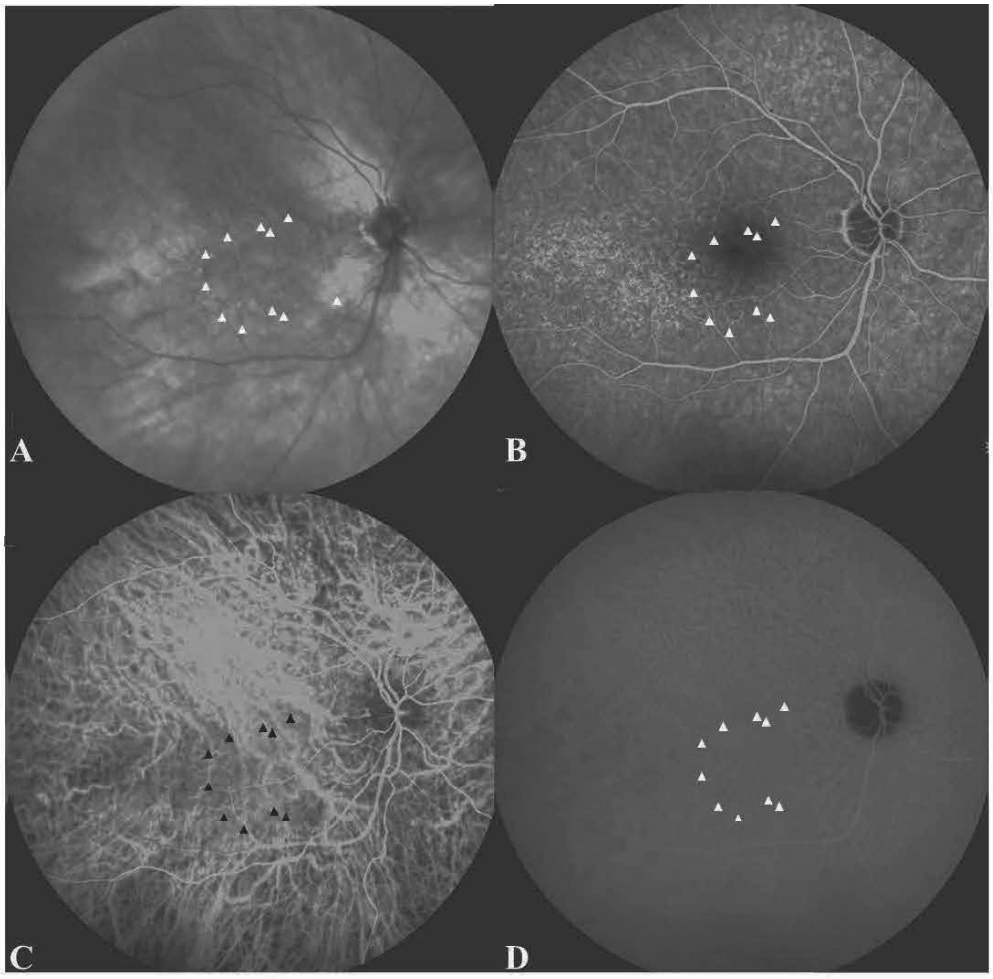

Figure S3. Retinal angiographic findings in a 51-year-old patient. (A) Near infra-red reflectance image demonstrating reticular pseudodrusen (RPD) (white arrowheads). (B) Late-phase fundus fluorescein angiogram shows temporal staining and masking of background fluorescence corresponding to the RPD. (C) Early indocyanine green angiography (ICGA) outlining choroidal vasculature. RPD (black arrowheads) are not clearly seen in early phase. (D) Late-phase ICGA shows masking of background choroidal fluorescence by RPD (white arrowheads).

Figure S4

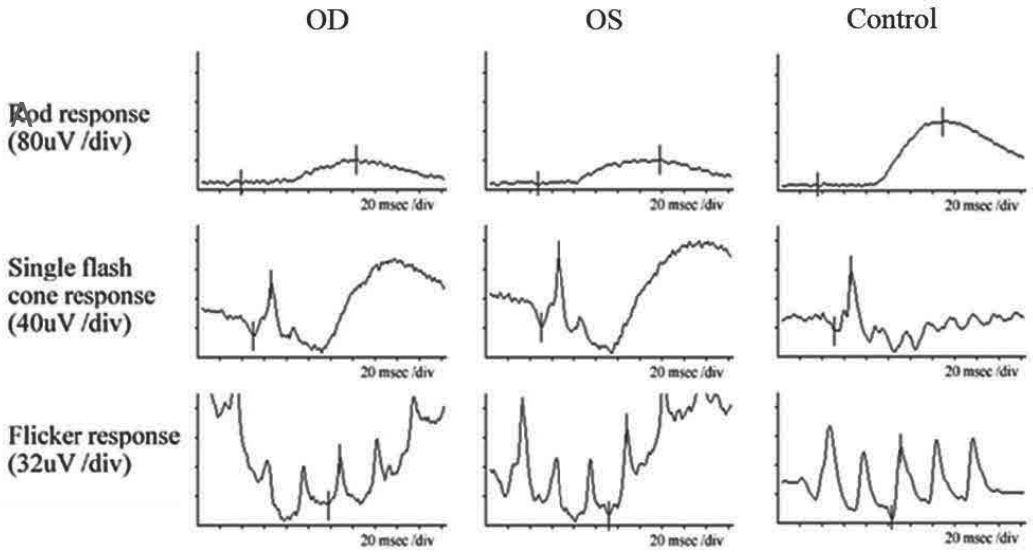

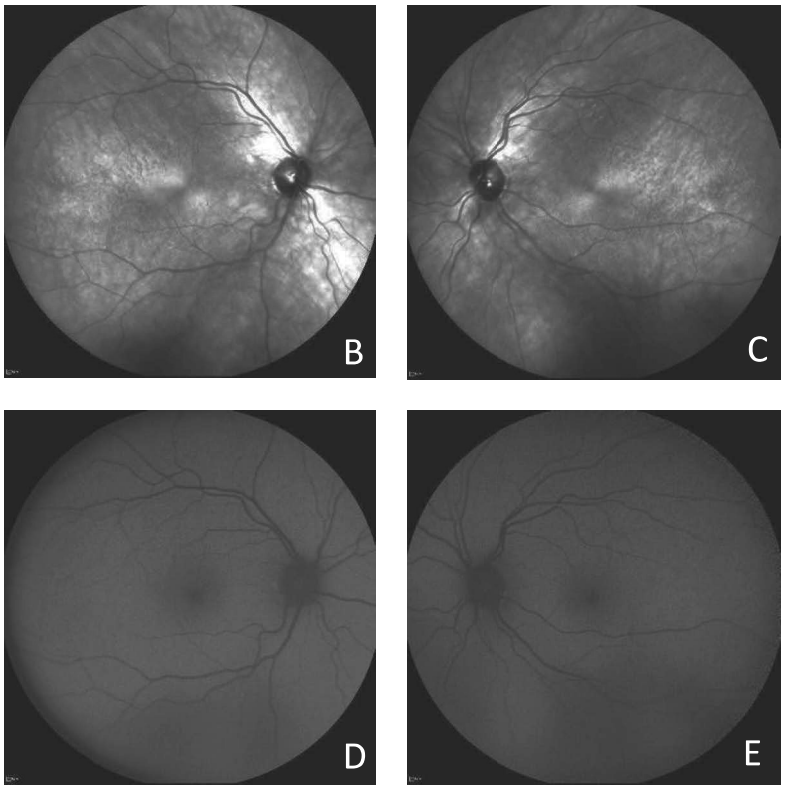

Figure S4. Full field electroretinography (ffERG) and imaging. The results of ffERG (A) in the 51-year-old patient from Figure 5C demonstrate a marked attenuation of rod responses after 20 minutes of dark adaptation with relative preservation of single flash and 30Hz flicker cone responses compared with the control. Near infra-red imaging (B and C) demonstrates reticular pseudodrusen. Bluelight autofluorescence imaging (D and E) shows that the is no marked atrophy present.

Table 1. Summary of late-onset retinal degeneration cohort patients investigated in this study. M=Male, F=Female, Y=Yes, N=No

Patient number	Sex (M/F)	Age at time of initial examination (years)	Baseline		Follow-up	
			Pseudodrusen right eye	Pseudodrusen left eye	Pseudodrusen right eye	Pseudodrusen left eye
1	M	60	Y	Y	N	N
2	M	56	Y	Y	Y	Y
3	F	68	Y	Y	Y	Y
4	F	68	Y	Y	Y	Y
5	F	60	Y	Y	Y	Y
6	M	47	N	Y	N	N
7	F	67	Y	Y	Y	Y
8	F	45	Y	Y	Y	Y
9	F	62	N	Y	N	Y
10	M	46	Y	Y	Y	Y
11	M	59	Y	Y	Y	Y
12	M	58	Y	Y	Y	Y
13	F	51	Y	Y	Y	Y
14	M	54	Y	Y	Y	Y
15	F	51	Y	Y	Y	Y
16	M	62	Y	Y	Y	Y
17	M	59	Y	Y	Y	Y
18	M	66	Y	Y	Y	Y
19	F	76	N	N	N	N
20	F	74	N	N	N	N
21	M	35	N	N	N	N
22	F	69	N	N	N	N
23	F	80	N	N	N	N
24	F	72	N	N	N	N
25	F	67	N	N	N	N
26	M	64	N	N	N	N
27	M	71	N	N	N	N
28	F	36	N	N	N	N
29	F	43	N	N	N	N